Atmos. Chem. Phys. Discuss., 11, 21171–21200, 2011
www.atmos-chem-phys-discuss.net/11/21171/2011/
doi:10.5194/acpd-11-21171-2011

Atmospheric Chemistry and Physics Discussions

Deposition freezing on mineral dust particles: a case against classical nucleation theory with the assumption of a single contact angle

M. J. Wheeler and A. K. Bertram

Department of Chemistry, University of British Columbia, Vancouver, BC CAN V6T 1Z1, Canada

Received: 21 June 2011 – Accepted: 7 July 2011 – Published: 27 July 2011

Correspondence to: A. K. Bertram (bertram@chem.ubc.ca)

Published by Copernicus Publications on behalf of the European Geosciences Union.

Abstract

Deposition freezing on two mineral species, kaolinite and illite, was studied using a flow cell coupled to an optical microscope at ~240 K. The results show that the onset S_{ice} (defined as the S_{ice} conditions when ice first nucleated) is a strong function of the surface area available for nucleation, varying from 100 % to 125 %. The surface area dependent data could not be described accurately using classical nucleation theory and the assumption of a single contact angle (defined here as the single-α model). These results suggest that caution should be applied when using contact angles determined from onset S_{ice} data and the single-α model. In contrast to the single-α model, the active site model, the deterministic model, and a model with a normal distribution of contact angles fit the data within experimental uncertainties. Parameters from the fits to the data are presented.

1 Introduction

Atmospheric aerosol particles can indirectly influence climate by modifying the formation conditions and properties of ice and mixed-phase clouds. To better understand this topic, an improved understanding of the ice nucleation properties of atmospheric aerosols is required, and these properties need to be parametrized and incorporated in atmospheric models (Baker and Peter, 2008; Cantrell and Heymsfield, 2005; DeMott, 2002; Hegg and Baker, 2009; Houghton et al., 2001).

Ice nucleation may occur in the atmosphere either homogeneously or heterogeneously. Homogeneous nucleation involves the freezing of liquid droplets. In heterogeneous nucleation, ice forms on insoluble or partially soluble aerosol particles known as ice nuclei (IN). Four different modes of heterogeneous ice nucleation have been identified: immersion, condensation, deposition and contact nucleation. In the following we focus on deposition nucleation, which involves the formation of ice on a solid particle directly from the vapour phase (Pruppacher and Klett, 1997; Vali, 1985).

ACPD
11, 21171–21200, 2011

Different theories or models have been developed to parametrize heterogeneous nucleation data. One of the simplest is classical nucleation theory (Pruppacher and Klett, 1997) combined with the assumption of a single contact angle, α. We refer to this as the single-α model. This model assumes ice nucleation is a stochastic process and can occur at any location on the surface of a particle with equal probability (i.e. the surface is energetically uniform for ice nucleation). Therefore, each particle has the same probability per unit surface area to nucleate ice (Pruppacher and Klett, 1997). Nucleation data is parametrized using a single parameter, the contact angle. Due in part to its simplicity, often researchers (including ourselves) have used the single-α model to parametrize laboratory data for use in atmospheric simulations (see for example: Archuleta et al., 2005; Chen et al., 2008; Chernoff and Bertram, 2010; Eastwood et al., 2008, 2009; Fornea et al., 2009; Hung et al., 2003). In addition, the single-α model has been used to describe heterogeneous nucleation in atmospheric cloud simulations (see for example: Hoose et al., 2010a,b; Jensen and Toon, 1997; Jensen et al., 1998; Kärcher, 1996, 1998; Kärcher et al., 1998; Morrison et al., 2005).

A modification of the single-α model is the Probability Distribution Function-α model (PDF-α model) (Lüönd et al., 2010; Marcolli et al., 2007). Similar to the single-α model, this model assumes that ice nucleation is stochastic and can be described by classical nucleation theory. Nucleation can occur at any location on the surface of a particle with equal probability (i.e. the surface is energetically uniform for ice nucleation). However, the ice nucleation ability varies from particle to particle, which is described by a probability distribution function of contact angles, α. This model has recently been used to parametrize laboratory data of Marcolli et al. (2007) and Lüönd et al. (2010).

Yet another modification to the single-α model is the active site model (Fletcher, 1969; Gorbunov and Kakutkina, 1982; Han et al., 2002; Lüönd et al., 2010; Marcolli et al., 2007; Martin et al., 2001). In this model it is assumed that ice nucleation is a stochastic process and can be described by classical nucleation theory. However, small areas or sites on a particle may be more effective at nucleating ice than the remainder of the particle. The distribution and ice nucleation properties of these areas, referred

ACPD
11, 21171–21200, 2011

to as "active sites" govern the nucleating ability of a particle. The active site model has been used for parametrizing laboratory data and for describing ice nucleation in atmospheric models (Fletcher, 1969; Gorbunov and Kakutkina, 1982; Khvorostyanov and Curry, 2000, 2004, 2005, 2009; Kulkarni and Dobbie, 2010; Lüönd et al., 2010; Niedermeier et al., 2010; Saunders et al., 2010).

A final model used here is the deterministic model (Connolly et al., 2009; Lüönd et al., 2010). Unlike the other three models discussed above, this model is not based on classical nucleation theory. When applied to deposition freezing, the deterministic model assumes particles have a characteristic number density of surface sites, and ice forms immediately on a surface site upon reaching a definite ice saturation ratio. This model has been used recently to parametrize immersion nucleation data on mineral dusts (Connolly et al., 2009; Lüönd et al., 2010; Murray et al., 2011).

In the following we investigate deposition freezing of ice on illite and kaolinite particles, two minerals that are a significant fraction (up to 50 %) of atmospheric mineral dust (Claquin et al., 1999). Mineral dust particles can play an important role in atmospheric ice formation based on previous field measurements and modelling studies (see for example: Ansmann et al., 2008; Barahona et al., 2010; Cziczo et al., 2004; DeMott et al., 2003; Heintzenberg et al., 1996; Hoose et al., 2008; Klein et al., 2010; Koehler et al., 2010; Li and Min, 2010; Min et al., 2009; Prenni et al., 2009; Sassen, 2002; Sassen et al., 2003; Seifert et al., 2010; Twohy and Poellot, 2005). We show that the onset S_{ice} values for freezing on kaolinite and illite particles are a strong function of the surface area available for nucleation (onset S_{ice} values are defined here as the S_{ice} conditions for the first appearance of ice nucleation). This surface area dependent data is then used to test the different models discussed above. We show that the single-α model cannot describe the laboratory data, but the PDF-α model, the active site model and the deterministic model fit the data within experimental uncertainties. Parameters from the fits to the data are presented and the atmospheric implications are discussed.

ACPD
11, 21171–21200, 2011

2 Experimental

2.1 Ice nucleation experiments

The apparatus used in these studies has been described in detail previously (Dymarska et al., 2006; Eastwood et al., 2008; Parsons et al., 2004). It consists of an optical microscope coupled to a flow cell in which the saturation ratio and temperature can be accurately controlled. The saturation ratio, S_{ice}, is defined as the ratio of water vapour partial pressure to the saturation vapour pressure of ice at the same temperature. Mineral dust particles were deposited on the bottom surface of the flow cell; the saturation ratio with respect to ice (S_{ice}) inside the cell was increased, and the conditions for onset of ice nucleation (when the first particle nucleated ice) was determined with a reflected light microscope. As mentioned, this is defined as the onset S_{ice}. The S_{ice} over the particles was controlled by continuously flowing a mixture of dry and humidified He through the flow cell. The bottom surface of the flow cell, which supported the particles, consisted of a glass cover slide treated with dichlorodimethylsilane to make a hydrophobic surface. This ensured that ice did not nucleate directly on the surface of the glass slide. The S_{ice} conditions at which all the particles nucleated ice could not be determined since after ice formed on the first particle, the S_{ice} above the other particles was reduced as water vapour condensed on the first nucleated particle.

Typical experimental S_{ice} trajectories used in these ice nucleation experiments are illustrated in Fig. 1. At the beginning of the experiments, the particles were exposed to a flow of dry He gas at room temperature ($S_{ice} < 1\%$). The temperature of the cell was then rapidly lowered and the S_{ice} was set to approximately 80 %. The nucleation experiments were then conducted by steadily decreasing the temperature $\left(-0.1\,\mathrm{K\,min^{-1}}\right)$ and thus increasing the S_{ice}. The S_{ice} ramp rate was approximately $1\%\mathrm{min}^{-1}$.

ACPD
11, 21171–21200, 2011

2.2 Sample preparation

Kaolinte and illite particles were purchased from Fluka and the Clay Mineral Society, respectively. Both samples were used as provided without any processing. The mineral samples were deposited on the hydrophobic glass slide using the following technique: dry dust particles were placed in a glass vessel immersed in an ultrasonic bath. A flow of ultrahigh-purity N_2 was passed through the vessel, and vibrations from the ultrasonic bath caused the dust particles to be suspended in the flow of N_2. This flow was directed at the hydrophobic glass slide, and the dust particles were deposited on the slide by impaction.

2.3 Particle number, particle size and total surface area

In the freezing experiments the number of mineral particles on the slide ranged from 1 to ~ 1000. This number could be coarsely controlled by varying the amount of time a slide was held under the gas stream containing suspended dust particles. Although the number of particles on the slide varied significantly from one experiment to the next, the size distribution of particles remained approximately constant. The total surface area of the mineral dust deposited in any particular experiment ranged from 3.5×10^{-6} to $8 \times 10^{-3}\,\mathrm{cm}^2$. Surface area values were measured for each sample by extrapolating the 2-dimensional surface area determined with the optical microscope assuming a spherical particle shape.

In separate experiments, we determined the average size of the kaolinite and illite particles to be 8 µm and 11 µm, respectively. Size determination involved suspending the particles in water and then measuring the size with a static laser light scattering instrument (Malvern Mastersizer 2000).

ACPD
11, 21171–21200, 2011

3 Results

3.1 Onset S_{ice} as a function of surface area

The individual onset results obtained for kaolinite and illite particles are shown in Figs. 2a and 3a respectively. Each data point represents the onset conditions observed for a single sample of dust particles, and the error bars are calculated from the uncertainty in the measurement of S_{ice}. A total of 85 and 63 individual nucleation experiments were performed for kaolinite and illite, respectively. Measurements made with surface areas greater than $\sim 10^{-4}$cm^2 show both kaolinite and illite to be very good ice nuclei; nucleation occurred at supersaturations of less than 5 %. These results are consistent with previous measurements for both kaolinite and illite particles (Bailey and Hallett, 2002; Chernoff and Bertram, 2010; Eastwood et al., 2008; Kanji et al., 2008; Möhler et al., 2008a,b; Salam et al., 2006; Welti et al., 2009; Zimmermann et al., 2007, 2008). The measurements made at low surface coverage $\left(<10^{-4}\text{cm}^2\right)$, however, show a different trend than was seen for the high surface coverage. Onset values were observed over a broad range of saturation ratios (100 % to 125 %). The spread in onset values between different experiments is greater than the uncertainty in the measurement of S_{ice}.

Figures 2b and 3b show average onset values calculated from the data presented in Figs. 2a and 3a. To determine averages the data were binned as a function of surface area. The bin width was chosen to produce an equal number of points in each bin. The uncertainty in the onset values reported in Figs. 2b and 3b correspond to the 95 % confidence interval for the averages. As can be seen from the figure, there is a clear trend of increasing average onset saturation ratio with decreasing surface area. Kanji and Abbatt (2010) observed a similar trend in deposition freezing experiments.

ACPD
11, 21171–21200, 2011

3.2 Fraction of particles nucleated as a function of S_{ice}

As an alternative to plotting surface area, one can plot the fraction of particles nucleated in each experiment. This can be calculated by dividing 1 (the number of particles nucleated in any experiment) by the total number of particles available to nucleate ice. In Figs. 2c and 3c we show the fraction of particles nucleated as a function of S_{ice}. For these figures we calculated the total number of particles available to nucleate ice by dividing the total surface area available for nucleation by the surface area of a single particle (using the average particle diameter). Plots like the ones shown in Figs. 2c and 3c (referred to as the activity spectrum) are often useful for predicting freezing in the atmosphere. Also, the data need to be presented in this manner for a direct comparison with the PDF-α model, the active site model, and the deterministic model (see below). Figures 2c and 3c show an increase in fraction nucleated with increasing saturation ratio (S_{ice}) as expected.

4 Discussion

4.1 Single-α model

Classical nucleation theory (Pruppacher and Klett, 1997) relates the rate of heterogeneous ice nucleation (J_{het}, in units of $cm^{-2}s^{-1}$) to the energy barrier for ice embryo formation on the substrate surface:

$$J_{het} = J_0 \exp\left(-\frac{\Delta F^*_{act}}{kT}\right), \quad (1)$$

where ΔF^*_{act} is the activation barrier to ice nucleation, J_0 is the pre-exponential factor in $cm^{-2}s^{-1}$, k is the Boltzmann constant, and T is the temperature in degrees Kelvin.

ACPD
11, 21171–21200, 2011

The value of the activation barrier is given by

$$\Delta F^*_{\mathrm{act}} = \frac{16\pi\sigma^3_{i/v} f\left(m_{i/v}\right)}{3\left[N_i kT \ln S_{\mathrm{ice}}\right]^2}, \quad (2)$$

where $\sigma_{i/v}$ is the ice-vapour interfacial energy in $\mathrm{J\,cm^{-2}}$, N_i is the molecular concentration of ice in $\mathrm{cm^{-3}}$, S_{ice} is the saturation ratio over the particles and $f\left(m_{i/v}\right)$ is the contact parameter of the embryo on the surface. For particle radii significantly larger than the radius of the ice germ (a good approximation under our conditions), $f\left(m_{i/v}\right)$ can be described by the following equation:

$$f\left(m_{i/v}\right) = \frac{\left(2+m_{i/v}\right)\left(1-m_{i/v}\right)^2}{4}, \quad (3)$$

where $m_{i/v}$ is the cosine of the contact angle of the ice embryo on the particle surface (i.e. $m_{i/v} = \cos\alpha$, where α is the contact angle). The physical meaning of the contact angle is not well understood and it is often used as a means of parametrizing laboratory data.

Combining Eqs. (1) and (2), the overall equation for the heterogeneous nucleation rate is obtained,

$$J_{\mathrm{het}} = J_0 \exp\left\{-\frac{16\pi\sigma^3_{i/v}}{3kT\left[kTN_i \ln S_{\mathrm{ice}}\right]^2} f\left(m_{i/v}\right)\right\}. \quad (4)$$

The single-α model is based on classical nucleation theory and assumes that every particle has the same contact angle. The nucleation rate mentioned above can be related to the surface area available for nucleation in our experiment by the following equation:

$$J_{\mathrm{het}} = \frac{1}{A_{\mathrm{total}} t}, \quad (5)$$

ACPD
11, 21171–21200, 2011

where A_{total} is the total surface area of particles in cm^2 and t is the time scale of the measurements taken as 10s (Chernoff and Bertram, 2010; Eastwood et al., 2008). Equations (4) and (5) can be combined to give a relationship between saturation ratio required for nucleation of one particle and the surface area in the experiments:

$$\ln S_{ice} = \sqrt{\frac{16\pi\sigma_{i/v}^3 f\left(m_{i/v}\right)}{3kT\ln(A_{total}J_0 t)}}\frac{1}{N_i kT}. \quad (6)$$

In Figs. 2b and 3b (solid line) we have calculated S_{ice} as a function of A_{total} using Eq. (6) and different contact angles. In these calculations we used an interfacial energy of $1.065\times10^{-5}Jcm^{-2}$ (Pruppacher and Klett, 1997), a temperature of 242.5K (the temperature at which measurements were made), a pre-exponential factor of $10^{25}cm^{-2}s^{-1}$ (Fletcher, 1958, 1959; Pruppacher and Klett, 1997) and a molecular concentration of ice of $3.1\times10^{22}\,cm^{-3}$ (calculated from the molecular mass and density of ice (Lide, 2001)). Both the values of $\sigma_{i/v}$ and N_i are calculated for hexagonal ice. Recent findings have shown that cubic ice is formed preferentially for homogeneous nucleation (Murray and Bertram, 2006; Murray et al., 2005) but more information is needed to determine the polymorph of ice that is formed by heterogeneous freezing.

It can be seen in Figs. 2b and 3b that there is no single contact angle capable of accurately modelling the data. Measurements made at high surface areas are described by a low value of the contact angle ($\alpha\approx0.052$ (3°) for kaolinite and $\alpha\approx0.122$ (7°) for illite). Comparatively, the measurements made at the lowest surface areas are described by a much larger contact angle ($\alpha\approx0.244$ (14°) for kaolinite and $\alpha>0.244$ (14°) for illite).

The single-α model can also be used to predict the fraction of particles nucleated as a function of S_{ice} as in Figs. 2c and 3c. Equation (7) shows the relationship between fraction of particles nucleated and the heterogeneous nucleation rate (Pruppacher and

ACPD
11, 21171–21200, 2011

Klett, 1997):

$$\frac{N_f}{N_0} = 1 - \exp\left(-A_{\text{particle}} \int_{t_0}^{t} J_{\text{het}}(t)\mathrm{d}t\right), \tag{7}$$

where $\frac{N_f}{N_0}$ is the frozen fraction of particles, J_{het} is the heterogeneous nucleation rate and A_{particle} is the area of a single kaolinite or illite particle. Equations (7) and (4) can then be combined to give the following equation:

$$\frac{N_f}{N_0} = 1 - \exp\left\{-A_{\text{particle}} J_0 \exp\left[\frac{-16\pi\sigma_{i/v}^3 f\left(m_{i/v}\right)}{3k^3 N_i^2}\right] \int_{t_0}^{t} \frac{1}{[T(t)]^3 \left[\ln S_{\text{ice}}(t)\right]^2}\mathrm{d}t\right\}. \tag{8}$$

Shown in Figs. 2c and 3c are calculations of the fraction frozen as a function of S_{ice} using Eq. (8) and assuming a single contact angle. In these calculations the rate of change in temperature of $-0.1\,\mathrm{K\,min^{-1}}$ of the cooling stage was used to calculate the time dependent temperature and saturation ratio. This was repeated for several values of the contact angle, α (orange lines in Figs. 2c and 3c). Figures 2c and 3c also show that the single-α model cannot describe our experimental data.

4.2 PDF-α model

As mentioned above, the PDF-α model is a modification of the single-α model (Lüönd et al., 2010; Marcolli et al., 2007). This model assumes that a single contact angle can describe an individual particle but that a distribution of contact angles exists for an ensemble of particles. Assuming a normal distribution of contact angles, the fraction of frozen particles is given by

$$\frac{N_f}{N_0} = 1 - \int_0^{\pi} \exp\left[-J_{\text{het}}(\alpha) A_{\text{particle}} t\right] f(\alpha)\mathrm{d}\alpha, \tag{9}$$

where $\frac{N_f}{N_0}$ is the frozen fraction of particles, $J_{\text{het}}(\alpha)$ is the classical heterogeneous nucleation rate at a particular contact angle given by Eq. (4), A_{particle} is the surface area

ACPD
11, 21171–21200, 2011

of the particle, t is the observation time and $f(\alpha)$ is the normal probability distribution at a particular value of α. The value $f(\alpha)\mathrm{d}\alpha$ is the fraction of particles having a contact angle between α and $\alpha + \mathrm{d}\alpha$. The normal probability distribution is described by the following equation:

$$f(\alpha) = \frac{1}{\sigma\sqrt{2\pi}}\left[-\frac{(\alpha-\bar{\alpha})^2}{2\sigma^2}\right], \quad (10)$$

where $\bar{\alpha}$ and σ are the mean and standard deviation of the distribution, respectively.

The blue lines in Figs. 2c and 3c show calculations of fraction frozen as a function of S_{ice} using the PDF-α model. The data was fit to the model by varying the parameters $\bar{\alpha}$, the mean contact angle, and σ, the width of the distribution of contact angles.

The best fit to the data (blue line in Fig. 2c) gave a mean contact angle ($\bar{\alpha}$) of 0.3367 (19.3°) and a width (σ) of 0.0869 (5.0°). The fit to the illite data (blue line in Fig. 3c) gave a mean contact angle of 0.4282 (24.5°) and a width of 0.1394 (8.0°). The distribution of contact angles are shown (black lines) in Fig. 4 for kaolinite and Fig. 5 for illite. The good agreement with the experimental data (as can be seen from the overlap of the predictions with experimental uncertainty) in Figs. 2c and 3c suggests this method effectively describes our freezing data. Fit parameters along with the coefficient of determination can be found in Tables 1 and 2 for kaolinite and illite respectively.

Previously Marcolli et al. (2007) and Lüönd et al. (2010) used a log-normal distribution of contact angles rather than a normal distribution when using the PDF-α model. We have also fitted our data using a log-normal distribution of contact angles, but found the normal distribution provided a slightly better fit for both minerals.

4.3 Active site model

The third method used to fit the experimental data was the active site model, which is a modification of the single-α model that includes the existence of active sites (Fletcher, 1969; Gorbunov and Kakutkina, 1982; Han et al., 2002; Lüönd et al., 2010; Marcolli

ACPD
11, 21171–21200, 2011

et al., 2007). The equations presented here are the same as those presented by Lüönd et al. (2010).

This model assumes ice nucleation occurs on active sites. For consistency, we assume that the size of an active site is constant and equal to 6 nm^2 as done by Lüönd et al. (2010). This is calculated from the critical ice embryo size determined for homogeneous nucleation of liquid water at 239 K using classical nucleation theory. The active site model assumes that the probability of ice nucleation on an active site is defined by a contact angle, α_i, and this contact angle can vary from site to site.

Similar to Eq. (7) presented above, the probability of nucleation on a single active site with contact angle, α, is

$$p(\alpha) = 1 - \exp\left[-J_{\text{het}}(S_{\text{ice}}, \alpha) A_\alpha t\right], \tag{11}$$

where $p(\alpha)$ is the probability of freezing, $J_{\text{het}}(S_{\text{ice}}, \alpha)$ is the saturation and contact angle dependent heterogeneous nucleation rate given by Eq. (4), A_α is the area of the active site (6 nm^2) and t is the time of observation. Similarly, the probability that nucleation does not occur on a single active site with contact angle α is

$$\bar{p}(\alpha) = \exp\left[-J_{\text{het}}(S_{\text{ice}}, \alpha) A_\alpha t\right]. \tag{12}$$

The probability of freezing of a single particle is described by the following equation, which takes into account the assumptions that a single particle can have multiple active sites and active sites can have a range of contact angles:

$$p(S_{\text{ice}}) = 1 - \prod_{i=1}^{m} \bar{p}(\alpha_i) = 1 - \prod_{i=1}^{m} \exp\left[-J_{\text{het}}(S_{\text{ice}}, \alpha_i) A_{\alpha_i} t\right], \tag{13}$$

where $p(S_{\text{ice}})$ is the probability of freezing of a single particle and $\bar{p}(\alpha_i)$ is the probability that an active site with a contact angle of α_i does not nucleate ice. A_{α_i} is the total surface area of active sites with a contact angle in the range $(\alpha_i, \alpha_i + \Delta\alpha)$ where $\Delta\alpha$ is the width of the individual bin such that the total number of bins is equal to m. A_{α_i} represents summation of all active sites within the specified range, each with

ACPD
11, 21171–21200, 2011

an area of 6 nm^2. Therefore, A_{α_i} is an integer multiple of the single active site area $\left(A_{\alpha_i} = n_i\left(6\text{nm}^2\right)\right)$.

The average number of active sites on a single particle in the range $(\alpha_i, \alpha_i + \Delta\alpha)$, $\bar{n}_i$, is given by

$$\bar{n}_i = 4\pi r^2 \rho(\alpha_i)\Delta\alpha, \tag{14}$$

where r is the radius of the particle and $\rho(\alpha)$ is the contact angle dependent surface density of active sites (i.e. number of active sites per unit surface area per unit contact angle interval). The number of active sites on a single particle, n_i, in the range $(\alpha_i, \alpha_i + \Delta\alpha)$, was assigned using Poisson distributed random variables with the expectation value given by Eq. (14). The n_i values determined from Poisson statistics were then used in Eq. (13) to determine the freezing probabilities, $p(S_{\text{ice}})$, of a single particle. This whole process was then repeated 10^5 times to determine freezing probabilities of an ensemble of 10^5 particles. The frozen fraction was then determined using the following equation:

$$\frac{N_f}{N_0} = \frac{1}{N_{\text{tot}}}\sum_{j=1}^{N_{\text{tot}}} p_j\left(S_{\text{ice}}\right), \tag{15}$$

where N_{tot} is the total number of particles $\left(10^5\right)$. As was done by Marcolli et al. (2007) and Lüönd et al. (2010), the surface density of active sites can be described using a three parameter exponential function of the following form:

$$\rho(\alpha) = b\exp\left(\frac{-\beta_1}{\alpha - \beta_2}\right). \tag{16}$$

The experimentally determined frozen fractions were fit to the active site model by varying the parameters, b, β_1, and β_2. Results are shown (green lines) in Figs. 2c and 3c for kaolinite and illite respectively. As can be seen in the figures, the active site model

ACPD
11, 21171–21200, 2011

provides a good fit to our experimental data. Fit parameters are reported in Tables 1 and 2 for kaolinite and illite respectively along with the corresponding coefficient of determination. Other values of the parameters were found which provided fits with R^2 values close to those reported in Tables 1 and 2. This was attributed to the low number of data points upon which the fits are based.

The fact that the experimental data is in agreement with the active site model is consistent with recent computer simulations of ice nucleation at the molecular level. These simulations show that the good ice nucleation characteristics of mineral dust is not likely due to the crystallographic match between mineral surface and hexagonal ice, but rather it is likely due to ice nucleation on defects such as trenches (Croteau et al., 2008, 2010; Hu and Michaelides, 2007).

4.4 Deterministic model

A final model used here is the deterministic model (Connolly et al., 2009; Lüönd et al., 2010). For deposition freezing as a function of S_{ice} and at a constant temperature (which is a reasonable approximation for our experiment) it is assumed that the particles have a surface density of active sites, $n_s(S_{ice})$, that become active on increasing the saturation ratio from 1 to S_{ice}. In addition it is assumed that the fraction of particles activated at a given S_{ice} is independent of time but related to $n_s(S_{ice})$ through the following equation:

$$\frac{N_f}{N_0} = 1 - \exp\left[-A_{particle} n_s(S_{ice})\right], \quad (17)$$

where $n_s(S_{ice})$ is the surface density of active sites at ~ 240 K and $A_{particle}$ is the surface area of a single particle. The surface density of active sites, $n_s(S_{ice})$, can be described by (Connolly et al., 2009; Lüönd et al., 2010),

$$n_s(S_{ice}) = \begin{cases} A_1 (S_{ice} + A_2)^2, & S_{ice} > -A_2 \\ 0, & S_{ice} \leq -A_2. \end{cases} \quad (18)$$

ACPD
11, 21171–21200, 2011

Using Eqs. (17) and (18), the experimentally determined frozen fractions were fit using the parameters A_1 and A_2. Good agreement was found between the experimental data and the deterministic model (red lines in Figs. 2c and 3c). Fit parameters can be found in Tables 1 and 2 for kaolinite and illite respectively along with the coefficient of determination.

4.5 Comparisons with previous measurements

Previous studies have also used various freezing data to test whether or not the single-α model can be used to accurately describe heterogeneous ice nucleation data for mineral dust particles. Several studies show that modifications to the single-α model are required for accurate predictions of heterogeneous freezing data (Archuleta et al., 2005; Hung et al., 2003; Lüönd et al., 2010; Marcolli et al., 2007; Welti et al., 2009). One exception is a recent study by Murray et al. (2011). This study investigated immersion freezing by kaolinite particles as a function of dust concentration and cooling rate. The data from this study were consistent with classical nucleation theory and the assumption of a single contact angle (the single-α model). The source of the kaolinite material used by Murray et al. was the Clay Mineral Society, which is a different source compared to our experiments. In addition, the work of Murray et al. investigated immersion freezing while our work examined deposition freezing. Future studies investigating the ice nucleation properties of different mineral sources may provide some insight into the apparent discrepancies.

5 Conclusions and atmospheric implications

Deposition freezing of ice on kaolinite and illite particles, two abundant minerals in the atmosphere, was investigated. The onset S_{ice} conditions for ice nucleation were a strong function of the surface area available for ice nucleation. For example, in the kaolinite experiments, average onset S_{ice} values ranged from 100 % to 125 % depending on the surface area used in the experiments.

The surface area dependent results were used to test the applicability of classical

ACPD
11, 21171–21200, 2011

nucleation theory with a single contact angle as a method to parametrize heterogeneous ice nucleation data. The surface area dependent data could not be described accurately using this model. These results add to the growing body of evidence that suggests that, in many cases, modifications to the single-α model are required for accurate predictions of heterogeneous freezing. The results also suggest that caution should be applied when using contact angles determined from the single-α model and onset data. This is because different contact angles can be derived from onset S_{ice} data and the single-α model depending on the surface area used in the experiments. As an example, the contact angle consistent with our onset S_{ice} data varied from 3° to >14° depending on the surface area. In contrast to the single-α model, the PDF-α model, the active site model and the deterministic model fit the data within experimental uncertainties. Parameters from the fits to the data are presented.

Acknowledgements. This research was supported by the National Sciences and Engineering Research Council of Canada (NSERC). We also thank Ben Murray for helpful comments on the manuscript.

References

Ansmann, A., Tesche, M., Althausen, D., Müller, D., Seifert, P., Freudenthaler, V., Hesse, B., Wiegner, M., Pisani, G., Knippertz, P., and Dubovik, O.: Influence of Saharan dust on cloud glaciation in southern Morocco during the Saharan mineral dust experiment, J. Geophys. Res., 113, D04210, doi:10.1029/2007JD008785, 2008. 21174

Archuleta, C. M., DeMott, P. J., and Kreidenweis, S. M.: Ice nucleation by surrogates for atmospheric mineral dust and mineral dust/sulfate particles at cirrus temperatures, Atmos. Chem. Phys., 5, 2617–2634, doi:10.5194/acp-5-2617-2005, 2005. 21173, 21186

Bailey, M. and Hallett, J.: Nucleation effects on the habit of vapour grown ice crystals from −18 to −42°C, Q. J. Roy. Meteor. Soc., 128, 1461–1483, 2002. 21177

Baker, M. B. and Peter, T.: Small-scale cloud processes and climate, Nature, 451, 299–300, doi:10.1038/nature06594, 2008. 21172

Barahona, D., Rodriguez, J., and Nenes, A.: Sensitivity of the global distribution of cirrus ice crystal concentration to heterogeneous freezing, J. Geophys. Res., 115, D23213, doi:10.1029/2010JD014273, 2010. 21174

ACPD
11, 21171–21200, 2011

Cantrell, W. and Heymsfield, A.: Production of ice in tropospheric clouds - A review, B. Am. Meteorol. Soc., 86, 795–807, doi:10.1175/BAMS-86-6-795, 2005. 21172
Chen, J.-P., Hazra, A., and Levin, Z.: Parameterizing ice nucleation rates using contact angle and activation energy derived from laboratory data, Atmos. Chem. Phys., 8, 7431–7449, doi:10.5194/acp-8-7431-2008, 2008. 21173
Chernoff, D. I. and Bertram, A. K.: Effects of sulfate coatings on the ice nucleation properties of a biological ice nucleus and several types of minerals, J. Geophys. Res., 115, D20205, doi:10.1029/2010JD014254, 2010. 21173, 21177, 21180
Claquin, T., Schulz, M., and Balkanski, Y. J.: Modeling the mineralogy of atmospheric dust sources, J. Geophys. Res., 104, 22243–22256, 1999. 21174
Connolly, P. J., Möhler, O., Field, P. R., Saathoff, H., Burgess, R., Choularton, T., and Gallagher, M.: Studies of heterogeneous freezing by three different desert dust samples, Atmos. Chem. Phys., 9, 2805–2824, doi:10.5194/acp-9-2805-2009, 2009. 21174, 21185
Croteau, T., Bertram, A. K., and Patey, G. N.: Adsorption and structure of water on kaolinite surfaces: possible insight into ice nucleation from grand canonical monte carlo calculations, J. Phys. Chem. A, 112, 10708–10712, doi:10.1021/jp805615q, 2008. 21185
Croteau, T., Bertram, A. K., and Patey, G. N.: Observations of high-density ferroelectric ordered water in kaolinite trenches using monte carlo simulations, J. Phys. Chem. A, 114, 8396–8405, doi:10.1021/jp104643p, 2010. 21185
Cziczo, D. J., DeMott, P. J., Brooks, S. D., Prenni, A. J., Thomson, D. S., Baumgardner, D., Wilson, J. C., Kreidenweis, S. M., and Murphy, D. M.: Observations of organic species and atmospheric ice formation, Geophys. Res. Lett., 31, L12116, doi:10.1029/2004GL019822, 2004. 21174
DeMott, P. J.: Laboratory Studies of Cirrus Cloud Processes, in: Cirrus, edited by Lynch, D. K., Sassen, K., Starr, D. O., and Stephens, G., pp. 102–136, Oxford University Press, New York, 2002. 21172
DeMott, P. J., Cziczo, D. J., Prenni, A. J., Murphy, D. M., Kreidenweis, S. M., Thomson, D. S., Borys, R., and Rogers, D. C.: Measurements of the concentration and composition of nuclei for cirrus formation, P. Natl. Acad. Sci. USA, 100, 14655–14660, doi:10.1073/pnas.2532677100, 2003. 21174
Dymarska, M., Murray, B. J., Sun, L. M., Eastwood, M. L., Knopf, D. A., and Bertram, A. K.: Deposition ice nucleation on soot at temperatures relevant for the lower troposphere, J. Geophys. Res., 111, D04204, doi:10.1029/2005JD006627, 2006. 21175

ACPD
11, 21171–21200, 2011

Eastwood, M. L., Cremel, S., Gehrke, C., Girard, E., and Bertram, A. K.: Ice nucleation on mineral dust particles: Onset conditions, nucleation rates and contact angles, J. Geophys. Res., 113, D22203, doi:10.1029/2008JD010639, 2008. 21173, 21175, 21177, 21180

Eastwood, M. L., Cremel, S., Wheeler, M., Murray, B. J., Girard, E., and Bertram, A. K.: Effects of sulfuric acid and ammonium sulfate coatings on the ice nucleation properties of kaolinite particles, Geophys. Res. Lett., 36, L02811, doi:10.1029/2008GL035997, 2009. 21173

Fletcher, N. H.: Size Effect in Heterogeneous Nucleation, J. Chem. Phys., 29, 572–576, 1958. 21180

Fletcher, N. H.: Entropy Effect in Ice Crystal Nucleation, J. Chem. Phys., 30, 1476–1482, 1959. 21180

Fletcher, N. H.: Active Sites and Ice Crystal Nucleation, J. Atmos. Sci., 26, 1266–1271, 1969. 21173, 21174, 21182

Fornea, A. P., Brooks, S. D., Dooley, J. B., and Saha, A.: Heterogeneous freezing of ice on atmospheric aerosols containing ash, soot, and soil, J. Geophys. Res., 114, D13201, doi:10.1029/2009JD011958, 2009. 21173

Gorbunov, B. Z. and Kakutkina, N. A.: Ice Crystal Formation on Aerosol Particles with a Non-Uniform Surface, J. Aerosol Sci., 13, 21–28, 1982. 21173, 21174, 21182

Han, J. H., Hung, H. M., and Martin, S. T.: Size effect of hematite and corundum inclusions on the efflorescence relative humidities of aqueous ammonium nitrate particles, J. Geophys. Res., 107, D104086, doi:10.1029/2001JD001054, 2002. 21173, 21182

Hegg, D. A. and Baker, M. B.: Nucleation in the atmosphere, Rep. Prog. Phys., 72, 056801, doi:10.1088/0034-4885/72/5/056801, 2009. 21172

Heintzenberg, J., Okada, K., and Ström, J.: On the composition of non-volatile material in upper tropospheric aerosols and cirrus crystals, Atmos. Res., 41, 81–88, 1996. 21174

Hoose, C., Lohmann, U., Erdin, R., and Tegen, I.: The global influence of dust mineralogical composition on heterogeneous ice nucleation in mixed-phase clouds, Environ. Res. Lett., 3, 025003, doi:10.1088/1748-9326/3/2/025003, 2008. 21174

Hoose, C., Kristjánsson, J. E., and Burrows, S. M.: How important is biological ice nucleation in clouds on a global scale?, Environ. Res. Lett., 5, 024009, doi:10.1088/1748-9326/5/2/024009, 2010a. 21173

Hoose, C., Kristjánsson, J. E., Chen, J.-P., and Hazra, A.: A classical-theory-based parameterization of heterogeneous ice nucleation by mineral dust, soot, and biological particles in a global climate model, J. Atmos. Sci., 67, 2483–2503, doi:10.1175/2010JAS3425.1, 2010b.

ACPD
11, 21171–21200, 2011

21173
Houghton, J. T., Ding, Y., Griggs, D. J., Noguer, M., van der Linden, P. J., Dai, X., Maskell, K., and Johnson, C. A. E.: IPCC, 2001: Climate Change 2001: The Scientific Basis. Contribution of Working Group I to the Third Assessment Report of the Intergovernmental Panel on Climate Change, Cambridge University Press, Cambridge UK, and New York., 2001. 21172
Hu, X. L. and Michaelides, A.: Ice formation on kaolinite: Lattice match or amphoterism?, Surf. Sci., 601, 5378–5381, doi:10.1016/j.susc.2007.09.012, 2007. 21185
Hung, H. M., Malinowski, A., and Martin, S. T.: Kinetics of heterogeneous ice nucleation on the surfaces of mineral dust cores inserted into aqueous ammonium sulfate particles, J. Phys. Chem. A, 107, 1296–1306, doi:10.1021/jp021593y, 2003. 21173, 21186
Jensen, E. J. and Toon, O. B.: The potential impact of soot particles from aircraft exhaust on cirrus clouds, Geophys. Res. Lett., 24, 249–252, 1997. 21173
Jensen, E. J., Toon, O. B., Pueschel, R. F., Goodman, J., Sachse, G. W., Anderson, B. E., Chan, K. R., Baumgardner, D., and Miake-Lye, R. C.: Ice crystal nucleation and growth in contrails forming at low ambient temperatures, Geophys. Res. Lett., 25, 1371–1374, 1998. 21173
Kanji, Z. A. and Abbatt, J. P. D.: Ice nucleation onto Arizona test dust at cirrus temperatures: effect of temperature and aerosol size on onset relative humidity, J. Phys. Chem. A, 114, 935–941, doi:10.1021/jp908661m, 2010. 21177
Kanji, Z. A., Florea, O., and Abbatt, J. P. D.: Ice formation via deposition nucleation on mineral dust and organics: dependence of onset relative humidity on total particulate surface area, Environ. Res. Lett., 3, 025004, doi:10.1088/1748-9326/3/2/025004, 2008. 21177
Kärcher, B.: Aircraft-generated aerosols and visible contrails, Geophys. Res. Lett., 23, 1933–1936, 1996. 21173
Kärcher, B.: Physicochemistry of aircraft-generated liquid aerosols, soot, and ice particles – 1. Model description, J. Geophys. Res., 103, 17111–17128, 1998. 21173
Kärcher, B., Busen, R., Petzold, A., Schröder, F. P., Schumann, U., and Jensen, E. J.: Physicochemistry of aircraft-generated liquid aerosols, soot, and ice particles – 2. Comparison with observations and sensitivity studies, J. Geophys. Res., 103, 17129–17147, 1998. 21173
Khvorostyanov, V. I. and Curry, J. A.: A new theory of heterogeneous ice nucleation for application in cloud and climate models, Geophys. Res. Lett., 27, 4081–4084, 2000. 21174
Khvorostyanov, V. I. and Curry, J. A.: The theory of ice nucleation by heterogeneous freezing of deliquescent mixed CCN. Part I: Critical radius, energy, and nucleation rate, J. Atmos. Sci.,

ACPD
11, 21171–21200, 2011

61, 2676–2691, 2004. 21174
Khvorostyanov, V. I. and Curry, J. A.: The theory of ice nucleation by heterogeneous freezing of deliquescent mixed CCN. Part II: Parcel model simulation, J. Atmos. Sci., 62, 261–285, 2005. 21174
Khvorostyanov, V. I. and Curry, J. A.: Critical humidities of homogeneous and heterogeneous ice nucleation: Inferences from extended classical nucleation theory, J. Geophys. Res., 114, D04207, doi:10.1029/2008JD011197, 2009. 21174
Klein, H., Nickovic, S., Haunold, W., Bundke, U., Nillius, B., Ebert, M., Weinbruch, S., Schuetz, L., Levin, Z., Barrie, L. A., and Bingemer, H.: Saharan dust and ice nuclei over Central Europe, Atmos. Chem. Phys., 10, 10211–10221, doi:10.5194/acp-10-10211-2010, 2010. 21174
Koehler, K. A., Kreidenweis, S. M., DeMott, P. J., Petters, M. D., Prenni, A. J., and Möhler, O.: Laboratory investigations of the impact of mineral dust aerosol on cold cloud formation, Atmos. Chem. Phys., 10, 11955–11968, doi:10.5194/acp-10-11955-2010, 2010. 21174
Kulkarni, G. and Dobbie, S.: Ice nucleation properties of mineral dust particles: determination of onset RH*i*, IN active fraction, nucleation time-lag, and the effect of active sites on contact angles, Atmos. Chem. Phys., 10, 95–105, doi:10.5194/acp-10-95-2010, 2010. 21174
Li, R. and Min, Q.-L.: Impacts of mineral dust on the vertical structure of precipitation, J. Geophys. Res., 115, D09203, doi:10.1029/2009JD011925, 2010. 21174
Lide, D. R. (Ed.): CRC Handbook of Chemistry and Physics, CRC Press LLC, Boca Raton, USA, 82 Edn., 2001. 21180
Lüönd, F., Stetzer, O., Welti, A., and Lohmann, U.: Experimental study on the ice nucleation ability of size-selected kaolinite particles in the immersion mode, J. Geophys. Res., 115, D14201, doi:10.1029/2009JD012959, 2010. 21173, 21174, 21181, 21182, 21183, 21184, 21185, 21186
Marcolli, C., Gedamke, S., Peter, T., and Zobrist, B.: Efficiency of immersion mode ice nucleation on surrogates of mineral dust, Atmos. Chem. Phys., 7, 5081–5091, doi:10.5194/acp-7-5081-2007, 2007. 21173, 21181, 21182, 21184, 21186
Martin, S. T., Han, J. H., and Hung, H. M.: The size effect of hematite and corundum inclusions on the efflorescence relative humidities of aqueous ammonium sulfate particles, Geophys. Res. Lett., 28, 2601–2604, 2001. 21173
Min, Q.-L., Li, R., Lin, B., Joseph, E., Wang, S., Hu, Y., Morris, V., and Chang, F.: Evidence of mineral dust altering cloud microphysics and precipitation, Atmos. Chem. Phys., 9, 3223–3231, doi:10.5194/acp-9-3223-2009, 2009. 21174

ACPD
11, 21171–21200, 2011

Möhler, O., Benz, S., Saathoff, H., Schnaiter, M., Wagner, R., Schneider, J., Walter, S., Ebert, V., and Wagner, S.: The effect of organic coating on the heterogeneous ice nucleation efficiency of mineral dust aerosols, Environ. Res. Lett., 3, 025007, doi:10.1088/1748-9326/3/2/025007, 2008a. 21177

Möhler, O., Schneider, J., Walter, S., Heymsfield, A. J., Schmitt, D., and Ulanowski, Z. J.: How coating layers influence the deposition mode ice nucleation on mineral particles, in: 15th Int. Conf. Clouds and Precipitation, Int. Comm. on Clouds and Precip., Cancun, Mexico, 2008b. 21177

Morrison, H., Curry, J. A., and Khvorostyanov, V. I.: A new double-moment microphysics parameterization for application in cloud and climate models. Part I: Description, J. Atmos. Sci., 62, 1665–1677, 2005. 21173

Murray, B. J. and Bertram, A. K.: Formation and stability of cubic ice in water droplets, Phys. Chem. Chem. Phys., 8, 186–192, doi:10.1039/b513480c, 2006. 21180

Murray, B. J., Knopf, D. A., and Bertram, A. K.: The formation of cubic ice under conditions relevant to Earth's atmosphere, Nature, 434, 202–205, doi:10.1038/nature03403, 2005. 21180

Murray, B. J., Broadley, S. L., Wilson, T. W., Atkinson, J. D., and Wills, R. H.: Heterogeneous freezing of water droplets containing kaolinite particles, Atmos. Chem. Phys., 11, 4191–4207, doi:10.5194/acp-11-4191-2011, 2011. 21174, 21186

Niedermeier, D., Hartmann, S., Shaw, R. A., Covert, D., Mentel, T. F., Schneider, J., Poulain, L., Reitz, P., Spindler, C., Clauss, T., Kiselev, A., Hallbauer, E., Wex, H., Mildenberger, K., and Stratmann, F.: Heterogeneous freezing of droplets with immersed mineral dust particles - measurements and parameterization, Atmos. Chem. Phys., 10, 3601–3614, doi:10.5194/acp-10-3601-2010, 2010. 21174

Parsons, M. T., Mak, J., Lipetz, S. R., and Bertram, A. K.: Deliquescence of malonic, succinic, glutaric, and adipic acid particles, J. Geophys. Res., 109, D06212, doi:10.1029/2003JD004075, 2004. 21175

Prenni, A. J., Petters, M. D., Kreidenweis, S. M., Heald, C. L., Martin, S. T., Artaxo, P., Garland, R. M., Wollny, A. G., and Pöschl, U.: Relative roles of biogenic emissions of Saharan dust as ice nuclei in the Amazon basin, Nat. Geosci., 2, 402–405, doi:10.1038/NGEO517, 2009. 21174

Pruppacher, H. R. and Klett, J. D.: Microphysics of Clouds and Precipitation, Atmospheric anc oceanographic sciences library, Kluwer Academic Publishers, Dordrecht, 2nd Edn., 1997. 21172, 21173, 21178, 21180

ACPD
11, 21171–21200, 2011

Salam, A., Lohmann, U., Crenna, B., Lesins, G., Klages, P., Rogers, D., Irani, R., MacGillivray, A., and Coffin, M.: Ice nucleation studies of mineral dust particles with a new continuous flow diffusion chamber, Aerosol Sci. Tech., 40, 134–143, doi:10.1080/02786820500444853, 2006. 21177

Sassen, K.: Indirect climate forcing over the western US from Asian dust storms, Geophys. Res. Lett., 29, 1465, doi:10.1029/2001GL014051, 2002. 21174

Sassen, K., DeMott, P. J., Prospero, J. M., and Poellot, M. R.: Saharan dust storms and indirect aerosol effects on clouds: CRYSTAL-FACE results, Geophys. Res. Lett., 30, 1633, doi:10.1029/2003GL017371, 2003. 21174

Saunders, R. W., Möhler, O., Schnaiter, M., Benz, S., Wagner, R., Saathoff, H., Connolly, P. J., Burgess, R., Murray, B. J., Gallagher, M., Wills, R., and Plane, J. M. C.: An aerosol chamber investigation of the heterogeneous ice nucleating potential of refractory nanoparticles, Atmos. Chem. Phys., 10, 1227–1247, doi:10.5194/acp-10-1227-2010, 2010. 21174

Seifert, P., Ansmann, A., Mattis, I., Wandinger, U., Tesche, M., Engelmann, R., Müller, D., Pérez, C., and Haustein, K.: Saharan dust and heterogeneous ice formation: Eleven years of cloud observations at the central European EARLINET site, J. Geophys. Res., 115, D20201, doi:10.1029/2009JD013222, 2010. 21174

Twohy, C. H. and Poellot, M. R.: Chemical characteristics of ice residual nuclei in anvil cirrus clouds: evidence for homogeneous and heterogeneous ice formation, Atmos. Chem. Phys., 5, 2289–2297, doi:10.5194/acp-5-2289-2005, 2005. 21174

Vali, G.: Nucleation Terminology, J. Aerosol Sci., 16, 575–576, 1985. 21172

Welti, A., Lüönd, F., Stetzer, O., and Lohmann, U.: Influence of particle size on the ice nucleating ability of mineral dusts, Atmos. Chem. Phys., 9, 6705–6715, doi:10.5194/acp-9-6705-2009, 2009. 21177, 21186

Zimmermann, F., Ebert, M., Worringen, A., Schütz, L., and Weinbruch, S.: Environmental scanning electron microscopy (ESEM) as a new technique to determine the ice nucleation capability of individual atmospheric aerosol particles, Atmos. Environ., 41, 8219–8227, doi:10.1016/j.atmosenv.2007.06.023, 2007. 21177

Zimmermann, F., Weinbruch, S., Schütz, L., Hofmann, H., Ebert, M., Kandler, K., and Worringen, A.: Ice nucleation properties of the most abundant mineral dust phases, J. Geophys. Res., 113, D23204, doi:10.1029/2008JD010655, 2008. 21177

ACPD
11, 21171–21200, 2011

Table 1. Fit parameters obtained for kaolinite. Best fits were obtained by minimizing the residual sum of squares between the experimental data and the fit function. See text for further discussion on the models used.

Model	Parameter	Value	R^2
PDF-α	$\bar{\alpha}$	0.3367	0.9961
	σ	0.0869	
Active site	b	$2 \times 10^{11} \mathrm{m}^{-2}$	0.9895
	β_1	0.5059	
	β_2	0.0172	
Deterministic	A_1	$1.08 \times 10^{11} \mathrm{m}^{-2}$	0.9927
	A_2	−1.008	

ACPD
11, 21171–21200, 2011

Table 2. Fit parameters obtained for illite. Best fits were obtained by minimizing the residual sum of squares between the experimental data and the fit function. See text for further discussion on the models used.

Model	Parameter	Value	R^2
PDF-α	$\bar{\alpha}$	0.4282	0.9979
	σ	0.1394	
Active site	b	$2 \times 10^{10} \mathrm{m}^{-2}$	0.9938
	β_1	0.3314	
	β_2	0.0045	
Deterministic	A_1	$1.92 \times 10^{10} \mathrm{m}^{-2}$	0.9976
	A_2	−0.977	

ACPD
11, 21171–21200, 2011

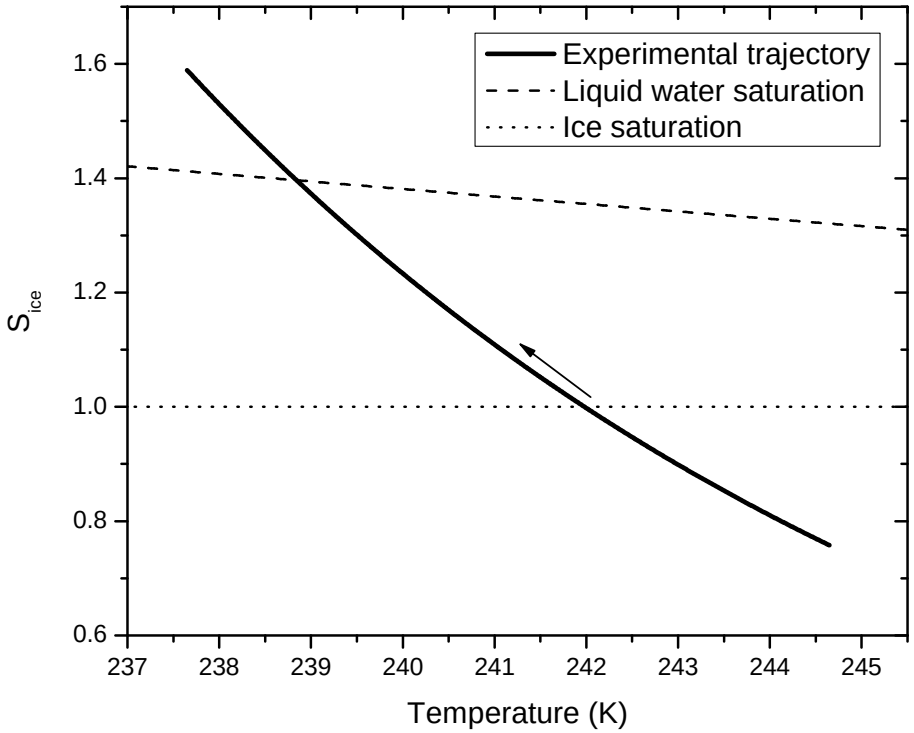

Fig. 1. Typical experimental trajectories for ice nucleation experiments. Experiments start below ice saturation and the temperature is decreased until ice crystals are observed.

ACPD
11, 21171–21200, 2011

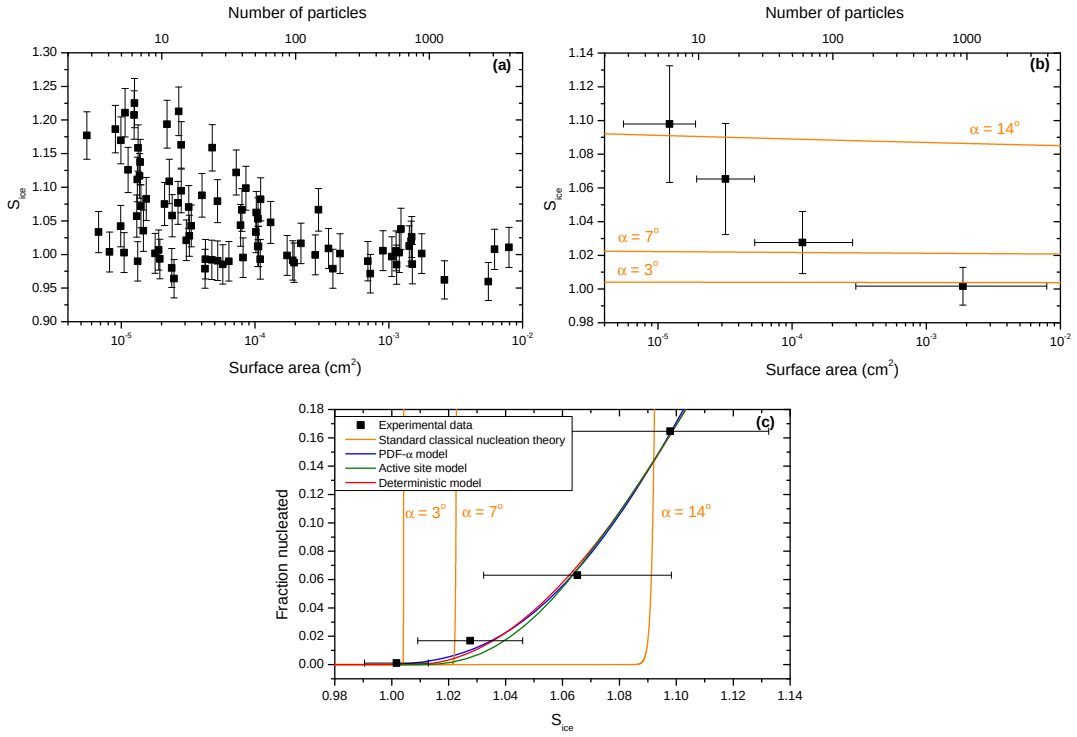

Fig. 2. Onset measurements for kaolinite particles of varying surface area showing **(a)** individual measurements, **(b)** average onset values and **(c)** fraction nucleated. The average values are calculated for four size ranges (range given as horizontal error bars in **(b)**). Error in S_{ice} is given as **(a)** experimental error in measurements of saturation and **(b)** and **(c)** 95 % confidence interval. Fits are shown using the single-α model **(b)** and **(c)** and using the PDF-α, active site and deterministic models in **(c)** only. In addition to surface area, **(a)** and **(b)** both show the corresponding number of particles calculated from the average particle size.

ACPD
11, 21171–21200, 2011

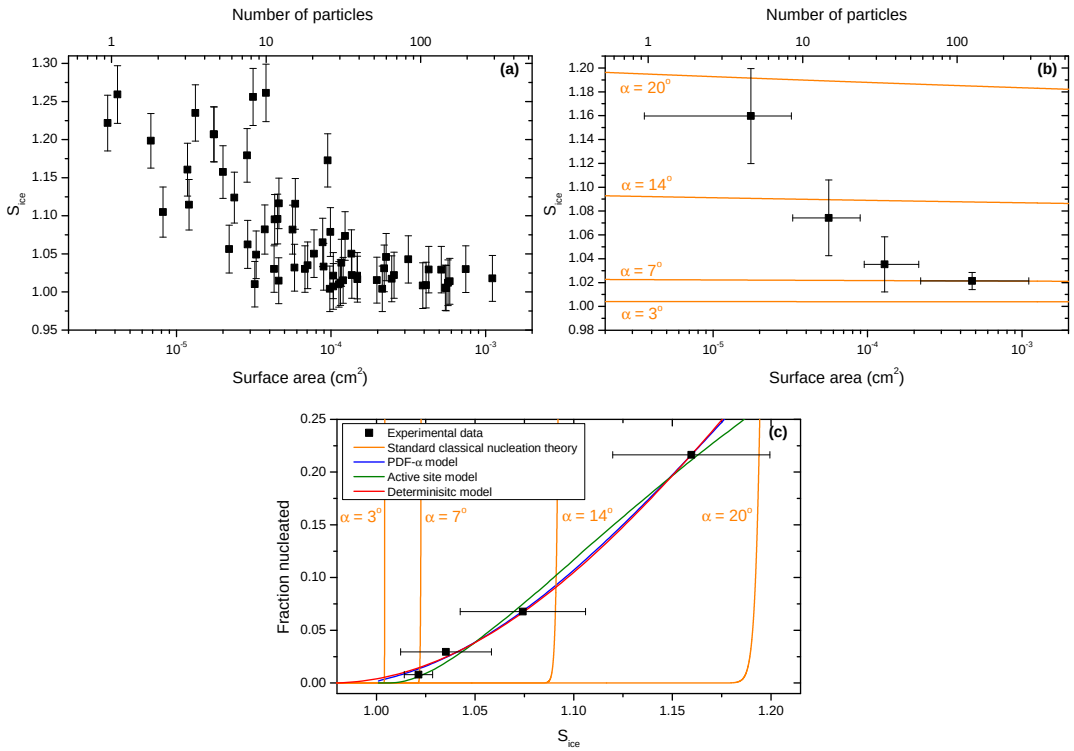

Fig. 3. Onset measurements for illite particles of varying surface area showing **(a)** individual measurements, **(b)** average onset values and **(c)** fraction nucleated. The average values are calculated for four size ranges (range given as horizontal error bars in **(b)**). Error in S_{ice} is given as **(a)** experimental error in measurements of saturation and **(b)** and **(c)** 95 % confidence interval. Fits are shown using the single-α model **(b)** and **(c)** and using the PDF-α, active site and deterministic models in **(c)** only. In addition to surface area, **(a)** and **(b)** both show the corresponding number of particles calculated from the average particle size.

ACPD
11, 21171–21200, 2011

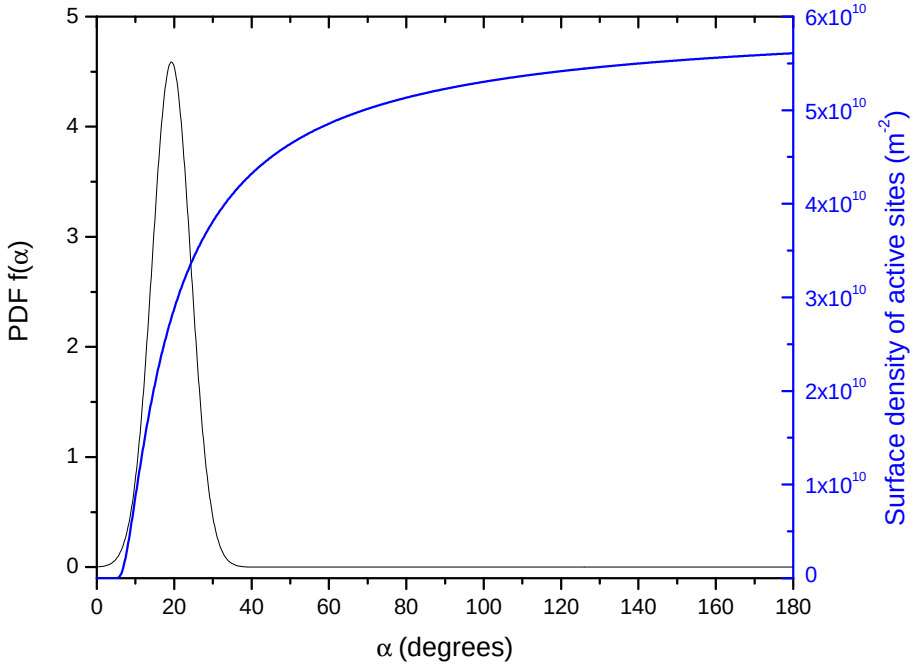

Fig. 4. Contact angle, α, distribution observed among kaolinite IN (black curve) for the α-PDF model and surface density of active sites (blue curve) per unit contact angle observed for the active site model.

ACPD
11, 21171–21200, 2011

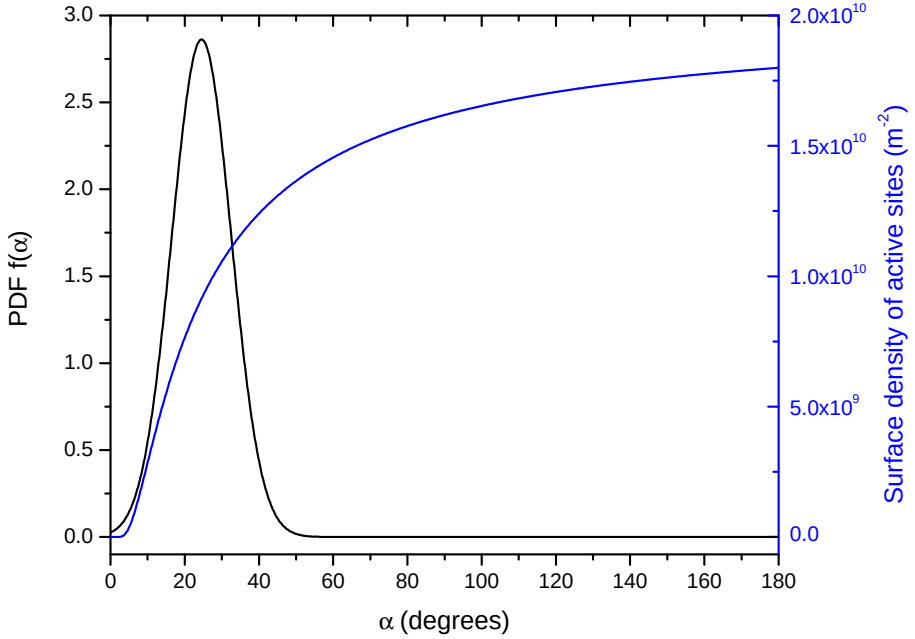

Fig. 5. Contact angle, α, distribution observed among illite IN (black curve) for the α-PDF model and surface density of active sites (blue curve) per unit contact angle observed for the active site model.

ACPD
11, 21171–21200, 2011